

Numerical model upgrading of a historical masonry building damaged during the 2016 Italian earthquakes: the case study of the Podestà palace in Montelupone (Italy)

F. Clementi¹ · A. Pierdicca¹ · A. Formisano²  · F. Catinari¹ · S. Lenci¹

Received: 20 July 2017 / Accepted: 8 October 2017 / Published online: 16 October 2017
© Springer-Verlag GmbH Germany 2017

Abstract In October 2016, two major earthquakes occurred in Marche region in the Centre of Italy, causing widespread damage. The epicentre of the second one struck Norcia, Visso and Accumoli and a lot of damages to cultural heritage were done in the cities of Tolentino, San Severino, Camerino, Matelica, Macerata and Montelupone, where are located the Podestà Palace and the Civic Tower investigated in this paper. The main aim of this research is the determination of modal properties of these historical masonry constructions using experimental and numerical studies. The experimental analysis was based on ambient vibration survey, while numerical analysis was based on finite element analysis with solid elements. The results of the experimental study were used to tune the numerical model of the structure. As the most doubtful parameters, the modulus of elasticity of the masonry and the interaction among structural parts were adjusted to achieve the experimental results with numerical model by simple operations. Obtaining good consistency between the experimental and numerical analyses, the study revealed the actual dynamic properties of the damaged palace.

Keywords Structural health monitoring · Cultural heritage · Masonry towers · Damage

1 Introduction

Cultural heritage (CH) buildings and sites represent an important historical and economic asset of European countries. In particular, Italy is characterized by a large number of CH structures. Moreover, European and especially Italian territories are characterized by a high seismicity and historical structures are constantly at risk. An enhanced knowledge of dynamic behaviour of structures can play a relevant role in defining proper countermeasures for existing buildings and historical structures.

The purpose to predict the performance of the building to different combinations of static and dynamic loads has attracted the interest of many researchers. Particularly, ambient vibration testing has become the main experimental method available for assessing the dynamic behaviour of full-scale structures [1], and this is especially true for CH because no excitation equipment is needed, involving a minimum interference with the normal use of the structure [2].

Ambient vibration testing permits to deduce dynamic properties of monitored structures, allowing a more specific and detailed intervention project. Dynamic monitoring allows preventing the execution of intrusive repair works, if they are not justified by an experimentally demonstrated worsening of the structural conditions [3, 4]. The Italian technical document Guidelines for evaluation and mitigation of seismic risk to CH [5], issued by the Ministry of Cultural Heritage and Activities and the Civil Protection Department, codify all these requirements. In this context, operational modal analysis (OMA) is increasingly acquiring relevance to evaluate the behaviour of civil structures in real ambient conditions. The main advantage of this technique is to measure the modal parameters of monitored

✉ A. Formisano
antoform@unina.it

¹ Department of Civil and Building Engineering, and Architecture (DICEA), Polytechnic University of Marche, Ancona, Italy

² Department of Structures for Engineering and Architecture, University of Naples Federico II, Naples, Italy

structures while they are operating in real ambient conditions, without artificial excitations.

In the present research, an experimental and numerical methodology is proposed, in order to perform the dynamic identification of a historical building lying in medium seismic hazard zones by using a wired sensor network. The measurements are performed with high sensitive piezoelectric sensors and data acquisition system, able to record ambient vibrations (AV) with very low amplitude range (10^{-6} m/s²).

One of the purposes of this work is to extract structural information about dynamic properties to complement an extensive research program planned to evaluate the structural condition of the tower, characterized by the presence of major cracks, especially on the walls between the tower and the palace. In this framework, the results of output-only modal identification tests can support the rational validation of the numerical model (NM), in particular for what concern the tower and its interaction with the palace, with some limits of the model definition and updating when referred only to palace (which will be eliminated once the structural safety of that area will be restored). Besides, the tuning of selected parameters makes possible the setting of a representative model of the structural behaviour in its current state [3, 6–8], in order to corroborate the damage and delimiting (to the best) the compromised area. Finite Element (FE) techniques have been shown to be an effective tool for the interpretation of physical behaviour of historic *fabrìca* [9–14]. In addition, as any damage changes the physical properties and, therefore, the modal response changes accordingly, a dynamic survey repeated over time combined with an FE model of the structure (able to assess the sensitivity of the modal parameters according to changes in the structural system) can be used for a structural health monitoring (SHM) [15–22], in particular following major aftershocks.

The historical structures are usually very challenging from the scientific and technical viewpoints because of their unique structural configurations and the large modelling uncertainties; for these reasons, a reliable model cannot be easily identified or cannot be identified at all [9, 23, 24]. Some uncertain parameters of the model, namely the Young's modulus of the masonry in different regions of the structure, were selected as "updating parameters" and iteratively modified to minimize the differences in the natural frequencies between FEA and OMA. Due to these complexities, an iterative procedure of FE model tuning is proposed in order to have a better perception on the structural behaviour alteration in the linear range.

The optimal model exhibits good agreement in both frequencies and mode shapes for all identified modes, provided that relatively low stiffness ratios were used in the

regions of the tower and palace where the major damage has been observed. Since the tower will be subjected to a repair intervention, a long-term goal [1, 21, 25] of this research is to repeat the dynamic tests after the strengthening in order to investigate the correlation between the repair and the changes in the modal parameters of the structure.

2 Basic preliminary information

The Podestà Palace (Fig. 1) is the most important building in the historic centre of Montelupone. A proper dating is not simple, considering that the first document from the Historical Municipal Archives, excluding some parchments, date back to the fifteenth century. Therefore, there are no reliable documents attesting to the date or the period of construction which, however, dates back to the end of the thirteenth century and the beginning of the fourteenth century. The building would be made by Lombard masters, for the markedly horizontal development, which it shares with the palace of the nearby Montecassiano town.

The actual palace is the result of the union of two distinct buildings (Fig. 2a). The project (Fig. 2b) was entrusted to architect Giuseppe Sabbatini at first. In his report, in 1894, he judged that the two round arches belonged to an earlier age than the three segmental arches. However, the works were only contracted in June 1910, based on the design of the engineer Ugo Cantalamessa (Fig. 2c), commissioned to complete the design of the porch, based on the previous project elaborated by Sabbatini. Other different retrofitting was made after the World War II, during which the palace suffered serious damage.

Between the end of the twentieth century and the beginning of the twenty-first century, some interventions at first level of the palace were done, like the substitution of the existing floor in the portion near the porch. Today, on



Fig. 1 Picture of the palace during the AVS in 2016 November 25th

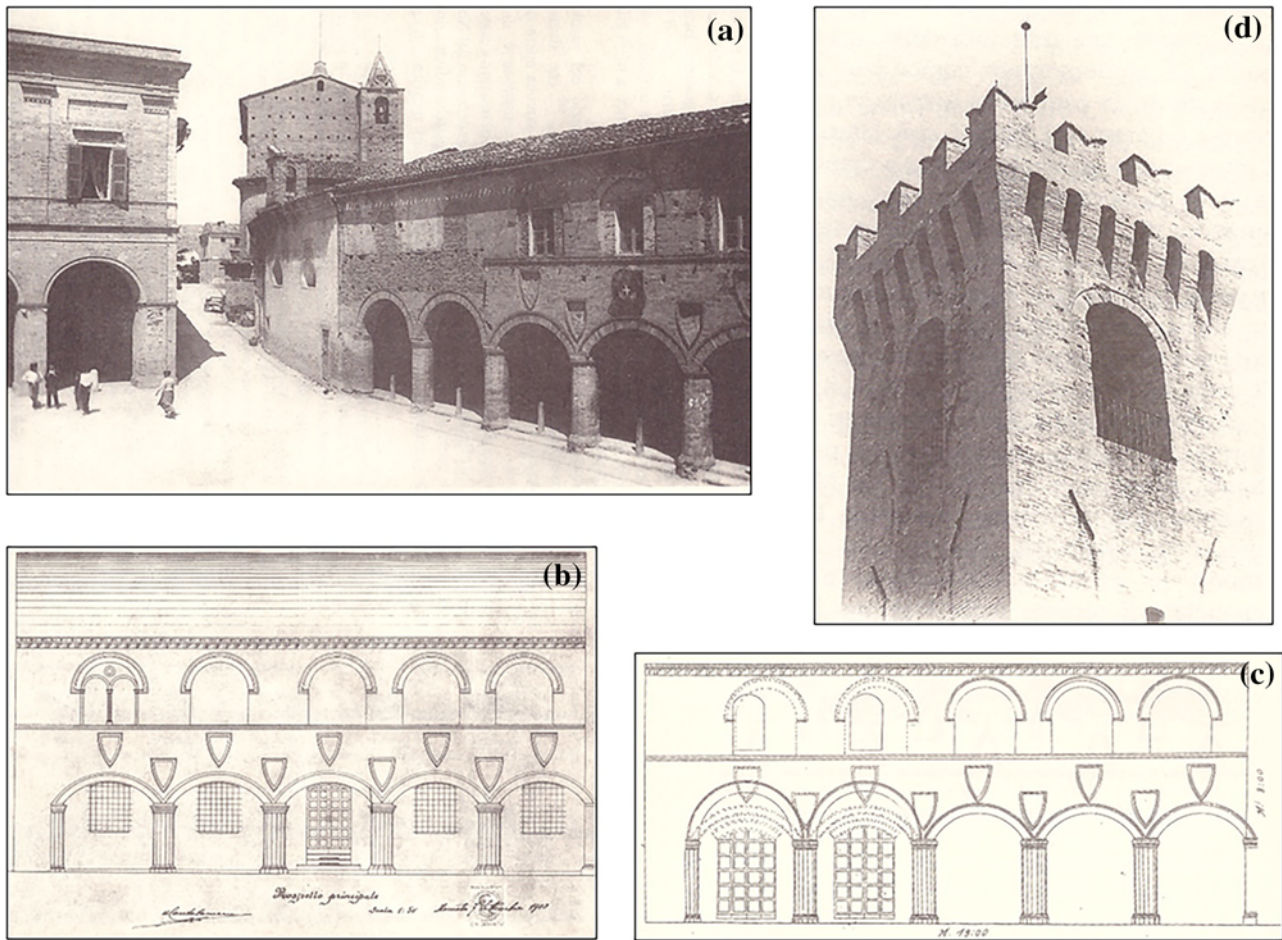


Fig. 2 The Podestà Palace at the end of the nineteenth century (a), facade of the Palace realized by Sabbatini (b) and Cantalamessa (c), conservation state of the tower in the mid of the nineteenth century (d)

the first floor the great hall has been transformed to an exhibition space, namely “Pinacoteca”, while on the ground floor, the two rooms are used as information point and office of the Municipal association.

Alongside the Podestà Palace stands the Civic Tower (Figs. 1, 2d). As for the palace, it is difficult to estimate the construction period, but it can be dated to the end of the twelfth century or the beginning of the thirteenth century.

Over the years, many retrofitting interventions, with the most important ones dated to the nineteenth century, were done. The tower was subjected to a series of important works for the installation of the new bell with a weight of 1521 kg, much heavier than the previous one, whose vibrations caused dangerous oscillations to the tower in the last decades, so to require the check of its stability. Other minor interventions were carried out over the past decades: in 2011, the old staircases inside the tower were replaced with steel stairs and some parapets were installed.

Finally, also the Piety Church is built in aggregate [26] within the Podestà Palace and dated back to the fourteenth century. It was an ancient church dedicated to St. John the

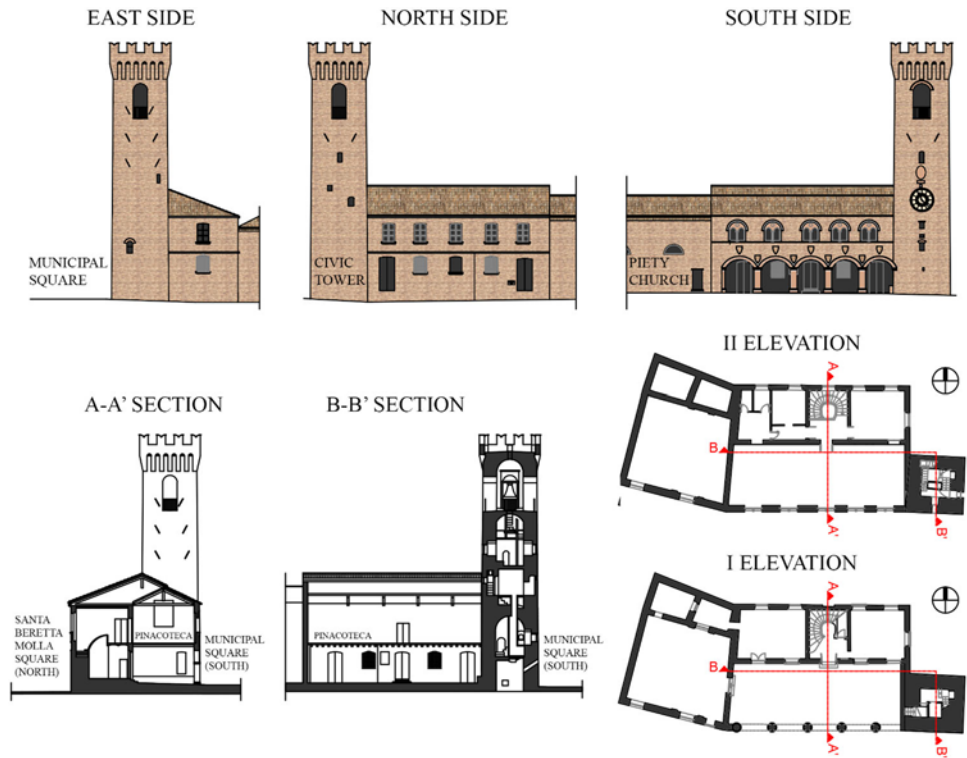
Baptist. Under Leo X pontificate, it became a church owned by the authority of the Canonises of Loreto and the seat of the Piety Confraternity. Today, the church is a municipal property and it has been used as temporary exhibitions halls.

The building occupies an area of about 35×16 m, with a height of about 11.8 m for the Podestà Palace and an average height of 26 m for the tower (Fig. 3). The structures are mainly made of masonry walls composed by solid bricks and lime mortar; the first and the roof levels of the church and palace are characterized by timber elements and arches. The walls thickness varies between 0.5 and 0.6 m passing from the palace to the church. At first glance, the floors are deformable due to a not correct link between the wooden elements and the concrete slab at the extrados of the palace first floor.

3 Damages due to 2016 earthquakes

On 2016 August 24th, the M_w 6.0 Amatrice earthquake [27–29] started a seismic sequence in the central Apennines that has lasted for months (and it is still ongoing at the

Fig. 3 Architectural fronts, transversal sections and plants of the palace, tower and Piety church



time of writing on July 2017), causing numerous casualties and damages to infrastructure [30]. The sequence has, so far, included two main shocks: the M_w 6.0 Amatrice earthquake and the M_w 6.5 Norcia earthquake, the latter being occurred on 2016 October 30th.

These main shocks have been accompanied by more than sixty thousand aftershocks–foreshocks including an M_w 5.9 event on 2016 October 26th [30]. The two main shocks (M_w 6.0 and 6.5) occurred at depths of between ~ 7 and ~ 9 km along the Mt. Gorzano Fault (MGF) and the Mt. Vettore Fault System (MVFS) in the central Apennines.

After the first seismic event of August 24th, the Podestà Palace was closed because several cracks appeared in the non-structural elements, especially in the *camorcanna* (i.e. light vaults made up of plaster and reed laths hanging from wooden centrings) [31] in some parts of the wooden roof of the palace (Fig. 4). The subsequent seismic event of October 30th produces a lot of damages in structural elements, as it is possible to observe comparing the Fig. 5a, acquired between August 25th and October 30th, and Fig. 5b, taken during the AVS of 2016 November 25th.

The most evident damages are focused on the first floor of the palace, in the contact area between the tower and the palace, where a normal-quality masonry and not good connections are observed. In particular, the tower pounded the walls of the “Pinacoteca” of the palace and a clear disconnection between the wall of the façades and the

tower appeared (Fig. 5b–f) in the interior and in the exterior facades, which actually are clearly visible.

At a first sight, the palace and the tower look simply close to each other, even if the detachment is visible only from a height of about 4 m (Fig. 5c). In fact, the palace and the tower are well connected up to the level of the arches at the base of the palace; meanwhile, the wall above seems to be of a normal quality and leaned on the tower.

Sliding between wooden roof beams and housing in the main walls have also appeared after the main shock (Fig. 4c). Further enlargements of the previous damages in stuccos and in *camorcanna* were observed. Actually, the Podestà Palace is closed and some retrofitting interventions should be addressed in order to reopen the building.

4 Ambient vibration testing on the building

The main objective of the present experimental campaign is the extraction of structural dynamic parameters, such as natural frequencies, damping ratios and mode shapes, and to detect the main damages after the three different earthquake events. The second goal, on the other hand, consists of tuning an NM of the building, which is need for the full understanding of the overall structural behaviour, to be later used for design retrofitting works. With this in mind, a preliminary, simple and not computationally expensive, NM of the structure was set up (starting from results



Fig. 4 Some damages in the *camorcanna* and in the connection between transversal walls (a), only in the *camorcanna* (b) and in the connection between wooden beams and walls of the facades (c)

obtained from the geometrical and architectural survey) and used to individuate some points on the building where the experimental tests had to be performed.

Experimental campaign has been performed and results of the dynamic experiments are then used to identify the uncertain parameters of the numerical model, i.e. those that were not possible to determine directly (for various reasons, including budget limitations and impossibility to perform semi-destructive tests) during the experimental campaign. Actually, the uncertain parameters have been selected as “updating parameters” and they are iteratively modified so that both main natural frequencies and corresponding mode shapes in the model match with the experimental ones.

4.1 Dynamic identification approach

Methods for vibration-based identification of modal parameters generally fall into two categories, depending on whether they operate in the time domain or in the frequency domain. However, the amount of information available is independent of whether the data are represented in the time or the frequency domain [32].

The method used in the presented work is in time domain, and it is based on a state-space description of the dynamic problem [33] using the Covariance Stochastic Subspace Identification (SSI-Cov) algorithm. In fact, the second-order problem, stated by the differential equation of motion, is converted into two first-order problems, defined by the so-called “state equation” and “observation equation.” Such equations, in the output-only case, can be written as follows for the generic discrete time instant $t = k\Delta t$, where Δt is the sampling period and $k \in \mathbb{N}$:

$$\{x_{k+1}\} = [A]\{x_k\} + \{w_k\} \quad (1)$$

$$\{y_k\} = [C]\{x_k\} + \{v_k\}, \quad (2)$$

where $\{x_k\} = \{x(k\Delta t)\}$ is the discrete time state vector yielding the sampled displacement and velocities, $\{y_k\}$ is the sampled output, $[A]$ is the discrete state matrix, $[C]$ is the discrete output matrix, $\{w_k\}$ is the “processed noise” due to disturbances and model inaccuracies, and $\{v_k\}$ is the “measurement noise” due to sensor inaccuracy. These vector signals are both immeasurable.

Using the procedure described in [34], once the state-space model has been constructed, the modal parameters (frequencies and damping ratios) can be extracted by the Eigen-decomposition of the system matrix $[A]$. To limit the length of the paper, the well-known algorithm formulation is not herein reported.

4.2 Equipment

The AV response of the tower and of the palace was measured at different elevations (see Fig. 6) and with different acquisitions. In particular, the AVs started with the acquisition of the tower only, by varying the layout of the accelerometers, and then continues with the acquisition of the tower and palace. The accelerometers were fixed directly in contact with the structural elements (Fig. 6) and parallel to the main directions of the building, in order to get both translational and torsional modes of the structure.

Each level was instrumented at least in two corners. At each corner, two high sensitive accelerometers, measuring in two orthogonal directions, were placed. Other couples of accelerometers were put in different positions at various

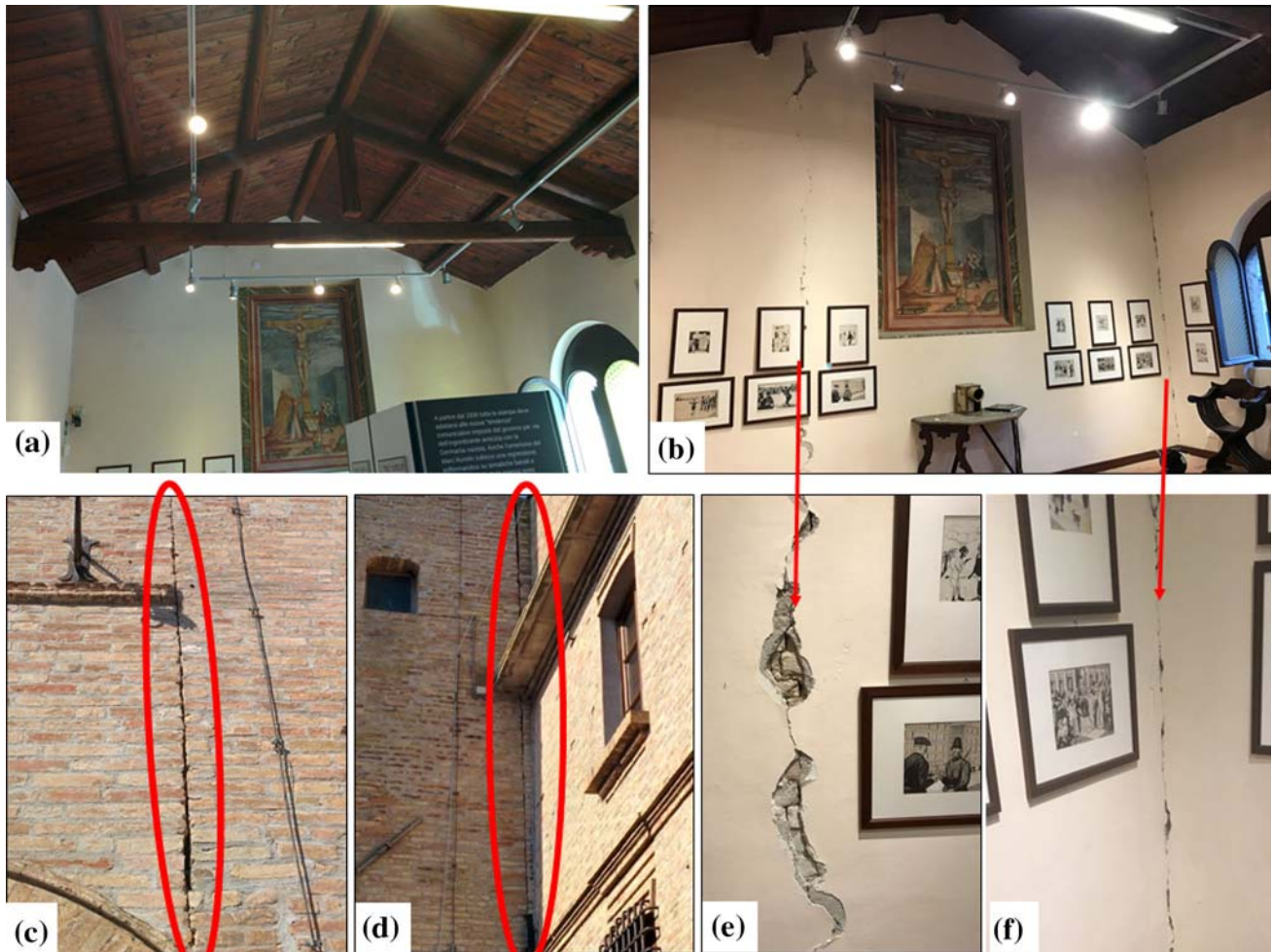


Fig. 5 Comparison of the main wall between the “Pinacoteca” and the tower before (a) and after (b) October 30th, where a clear disconnection is present in the north (c) and south (d) parts between

the facades and the tower. Some enlargements of the interior cracks are reported in the middle of the wall (e) and in the south façade (f)

levels in order to obtain more information about the dynamic behaviour of the whole structure. Regarding AVS of the palace, for safety issues, it was not possible to access to all area of the first floor but only to those in contact with the tower.

A wired sensor network was used, composed of two types of piezoelectric sensors (Integrated Electronic Piezoelectric—IEPE):

- KS48C-MMF with voltage sensitivity of 1 V/g and measurement range of ± 6 g (in blue in Fig. 6);
- KB12VD-MMF with voltage sensitivity if 10 V/g and measurement range of ± 0.6 g (in red in Fig. 6).

The digital recorder (DaTa500) is composed by a 24-bit Digital Signal Processor (DSP), an analogue anti-aliasing filter and a high-frequency acquisition range (0.2 Hz–200 kHz). RG58 coaxial cables link accelerometers and recorder. M28 and M32 signal conditioners with a frequency range of 0.1–100 kHz and selectable gain are also

used for each record. Some images of the instrumentation used for AVS are reported in Fig. 6.

4.3 Dynamic measurement and estimation of structural dynamic properties

The collected measurements were originally sampled at 1000 Hz. They were decimated by a factor of 40 before processing to have the ultimate data of 12.5 sample per second (SPS) [35].

The record duration varied between 40 min and 1 h: it should be long enough to eliminate the influence of possible non-stochastic excitations that may occur during the test [36]. The described procedure was used for each AVS.

A modal parameter extractor developed in Labview[®] programming language carried out data processing. It can perform analyses in time domain according to the SSI-Cov procedure mentioned before.

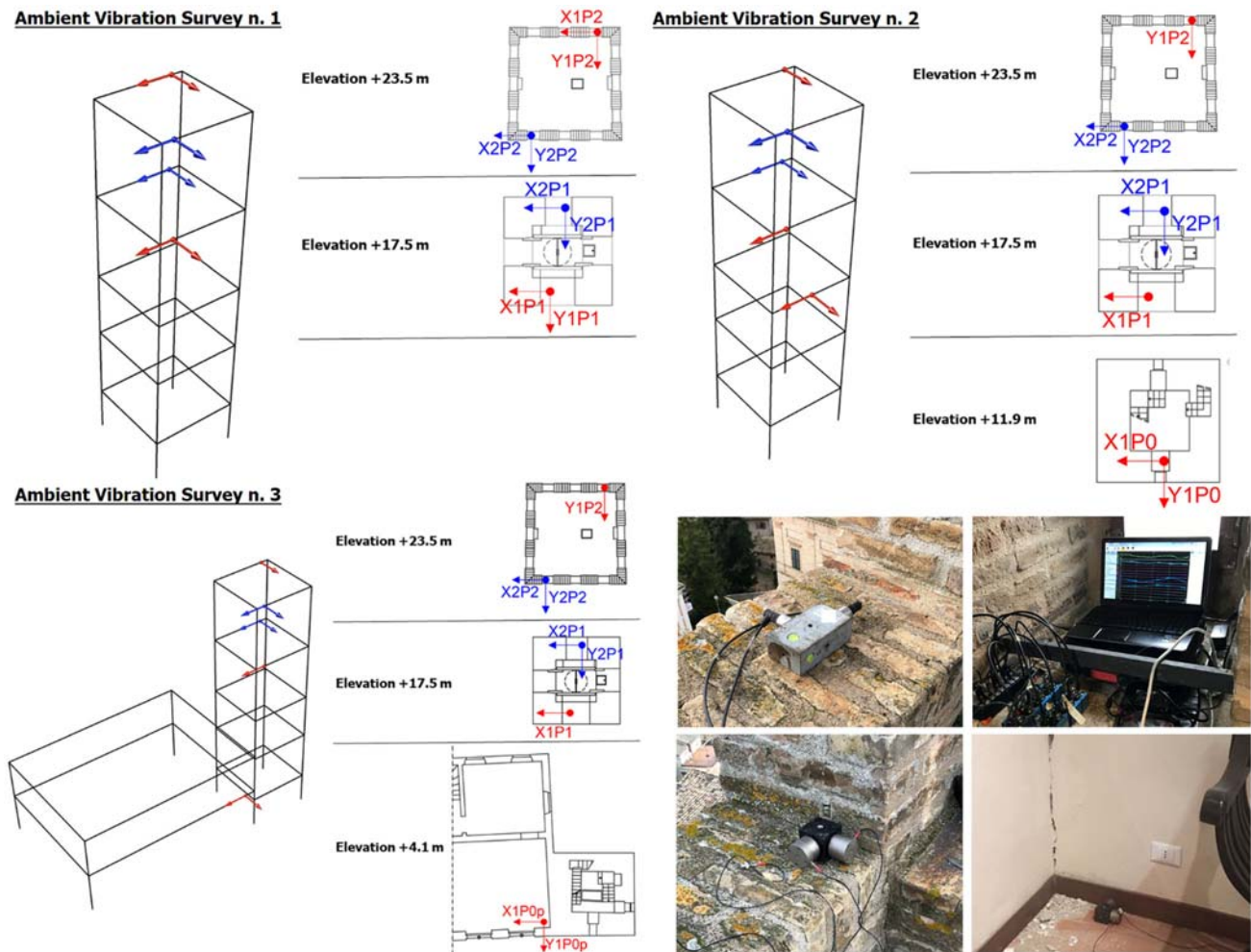


Fig. 6 Layout of the accelerometers at each floor (see online version for colours) for different ambient vibration surveys

The stabilization diagram obtained from the analysis of the collected data through Cov-SSI is reported in Fig. 7. It shows the alignments of stable poles, for increasing order models, and allows the determination of the “n” eigenvectors of dynamic matrix $[A]$ which are representative of structural modes, and how many are instead purely numeric (due to their redundancy of calculation or noise). Red points indicate negative results of the stability test; while green points represent the positive ones: considering that natural modes show intrinsic characteristics of the structure, they are invariant to the process and the order of the NM [37]. Then, it is possible to isolate the natural modes from the numerical ones by increasing the order of the model and checking the stability of the results.

The stability of a pole is defined as follows:

- the estimated frequency is considered stable if it does not change more than 2%;
- the damping for different orders should not deviate more than 15%;

- the modal shape obtained by a certain order is compared with the same obtained by a minor order by Modal Assurance Criterion (MAC) that must be at least equal to 90%. The modal identification results are reported in Table 1.

The identified frequencies appear rather spaced, the relative mode shapes mainly involve the tower and global modes appear only for values upper to the third (Fig. 7). In fact, the first three modes involve only the tower in particular: the 1st and 2nd modes are mixed translational modes involving the tower—at the same time—in X- and Y-directions. The torsional component is visible with the 3rd mode that always involves the tower in the upper part; lastly, the 4th mode involves the upper part of the tower and the first floor of the palace with an anti-phase translational movement.

Complexity plots may also be very useful to check if the shapes are normal or not [38]. A shape is called a “normal” shape if all of its shape components have 0 or 180 degrees

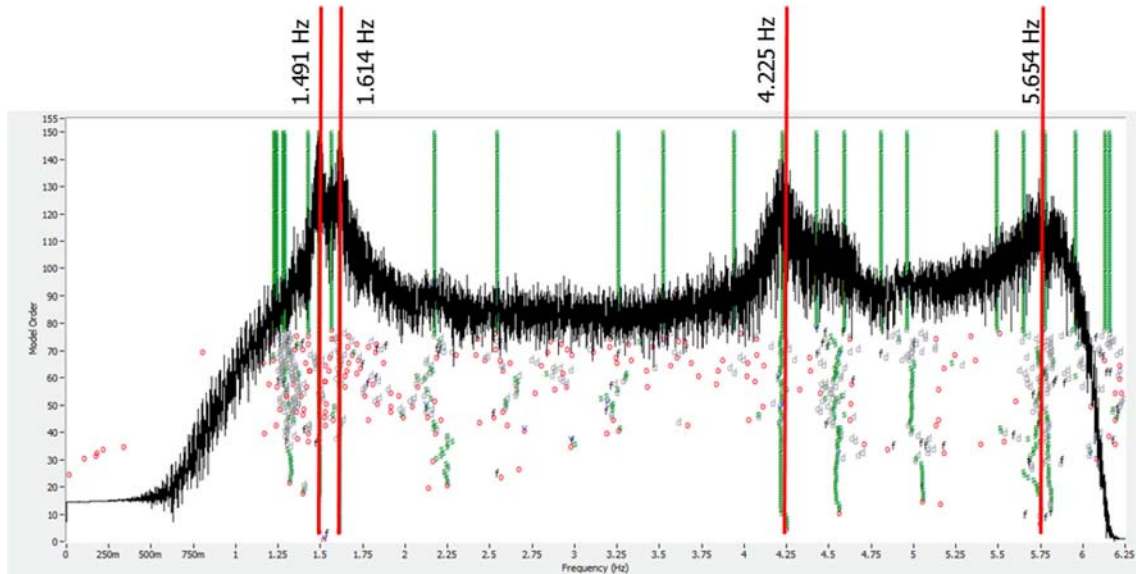


Fig. 7 Stabilization diagram (Cov-SSI) (see online version for colours)

Table 1 Modal shapes identified with the Cov-SSI technique

Mode number	Type	Natural frequency (Hz)	Damping ratio (%)
1	Translational X–Y	1.491	1.2
2	Translational X–Y	1.614	1.3
3	Torsional Z	4.225	1.2
4	Translational X–Y	5.654	2.5

of phase relative to one another. In other words, all the shape components lie along a straight line in the Complexity Plot. A “complex” shape can have arbitrary phases in its shape components, so they will not lie along a straight line. Figure 8 shows the complexity plots from the measurement data: all modes are normal or nearly normal (see, for instance, the third and fourth modes, which are weakly excited).

5 Finite element modelling of the building

A numerical 3D finite element (FE) model [39] of the structure was built using the commercial code MIDAS FEA®, where geometry was based on the results of a survey. In this study, as the aim of numerical modelling is to identify the linear dynamic behaviour of the building, the macro-modelling approach was used and the masonry was modelled as an isotropic continuum material. Masonry walls were modelled using 3D solid elements and particular attention was paid to reproduce their main geometric irregularities. All the openings of the building were reproduced together with the vaults and arches and wooden roofs were also modelled (Figs. 3, 9).

The NM was developed assuming a linear behaviour for the masonry because the small displacements framework is investigated, where the detected damage is due to the previous earthquakes and does not develop during the experimental campaign (a fact that would require more complex material modelling).

The final model reproduces with acceptable confidence (i.e. compared to the available data) the overall geometrical configuration of masonry walls together with the entire set of architectural elements of structural relevance. This attention is particularly required in historic buildings, where differences between architectural and structural elements are not always clear.

A relatively large number of finite elements were used in the model, which was formed by quadrilateral and tetrahedral elements with a maximum side equal to 0.30 m. Therefore, the model results in a total of 80349 nodes and 346806 elements with 235929 active degrees of freedom. A 3D view of the model is shown in Fig. 9.

The elastic parameters like Young’s modulus E , Poisson’s coefficient ν , and weight per unit volume γ are reported in Table 2 and should be considered as homogeneous in the structure. These values represent the starting point of our updating analysis, and they are chosen on the basis of what suggested by the Italian Code [40, 41] in

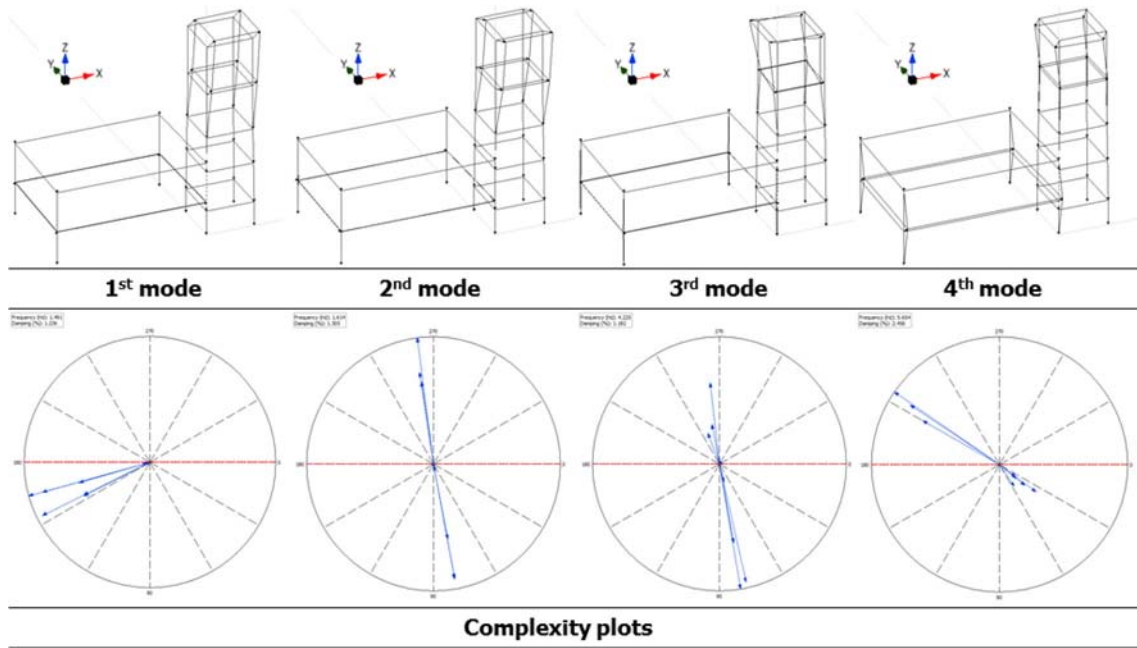
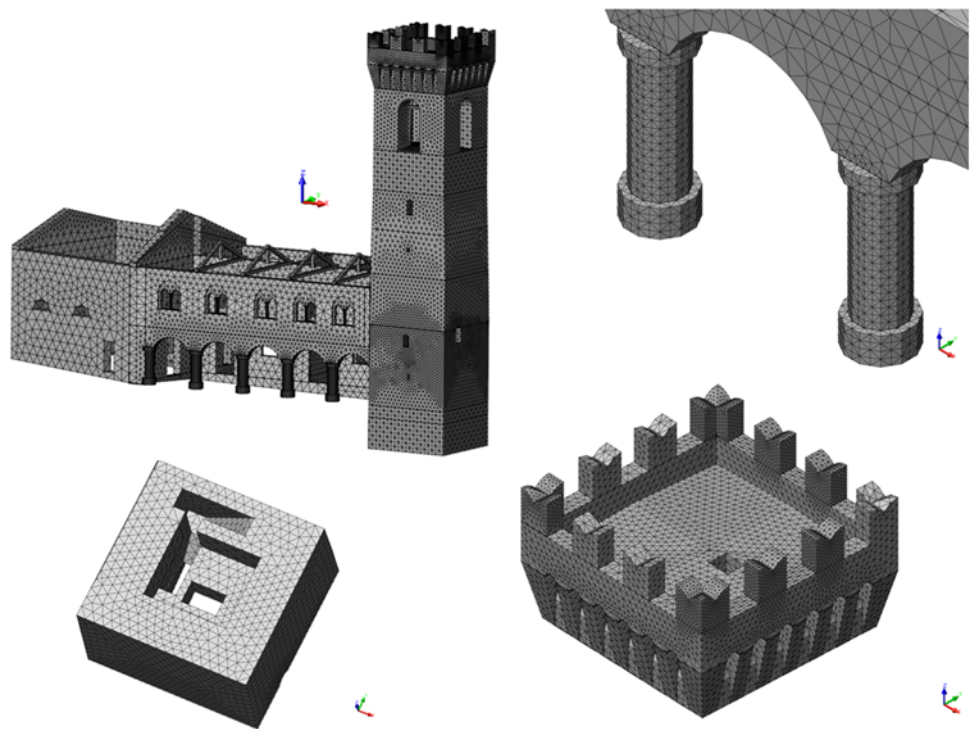


Fig. 8 Modal shapes identified with SSI technique (see online version for colours) and relative complexity plots

Fig. 9 View of the FE model of the structure and some structural details



Annex C8A.2, corresponding to a solid bricks with lime mortar.

Loads are defined according to the floor destination, following Italian provisions about loading conditions [40]. Masses are uniformly distributed on the slabs. If well connected to the walls, timber roof beams are directly modelled;

differently they are applied as loads only, as well as the structure bells.

5.1 Modal analysis of the structure: initial NM

The Lanczos method analysis was used to catch the main modes of the Podestà Palace, Piety Church and Tower. The

Table 2 Elastic parameters at the starting point of the calibration process

	E (MPa)	ν	γ (kN/m ³)
Solid bricks with lime mortar	1500	0.4	18

mass was directly transferred to the walls and the data reported in Fig. 9 and Table 2 are the starting points of this calibration work. The walls of the “Pinacoteca” are disconnected with respect to the tower in the second elevation according to the observed damages reported in Fig. 5c, d. Considering that the vast majority of modes involves small participation masses and local movements due to the lack of uniform rigid floors, more than 70 vibration modes were taken into account to achieve 85% of mass participation ratio.

The dynamic properties and mode shapes of the structure, reported in Table 3 and illustrated in Fig. 10, have revealed important characteristics of the structural behaviour. The first three modes reach about 30% of the mass participation ratio in X-direction and about 45% in Y-direction, involving separately the tower (the first two modes) and the Palace (the third mode). Differently, the fourth is the first mode that involves contemporary the palace and the tower. The subsequent modes, not reported in Table 3, are always local and involve the elements in out-of-plane deformations.

The main consideration, comparing the results of AVS in Fig. 8 and those of NM reported in Fig. 10, is that the structure has a clear decoupled dynamical behaviour between tower and palace. The main difference is that the third mode of AVS involves only the tower, while that of NM involves only the second level of the “Pinacoteca”. On the other hand, the frequencies are not scattered. To have a better understanding of this situation, a correlation analysis could be made in terms of scattering between analytical and experimental values of natural frequencies:

$$\Delta f [\%] = \left| \frac{f_i^e - f_i^a}{f_i^e} \right| 100, \tag{3}$$

where f_i^e is the experimental value and f_i^a is the analytical value of the natural frequency for the i th mode [6, 42].

Using Eq. (3), it is possible to observe that there is a quite small difference between the first three frequencies values as reported in Table 3 (last column): about + 3.75% for the first mode, – 2.08% for the second mode, – 1.0% for the third mode. The main difference is for the fourth mode, where a + 14.81% is observable comparing the experimental and the numerical frequencies.

6 Model updating procedure

Several identification methods are available to determine modal properties of structures. In the present study, instead of using one of the identification algorithms, the NM of *Podestà Palace* is updated by compare-alter-check based iterative solutions like those preliminary reported in [12]. The general modal and structural characteristics of the palace, such as high number of degree of freedom, possible variability in the material properties of masonry and limited number of measurements for AVS, prevent the use of those algorithms. In the iteration, the mode shapes and the frequencies of the structure, obtained by experimental and numerical surveys, are compared and Young’s modulus of masonry is updated at each subsequent step in order to reduce the frequencies scattering.

The calibration process consists of several steps as reported in [43]. In each step, mode shapes of NM are shown, calibration process is summarized and the results of the calibration are explained. It should be noted that the model upgrades itself after each step of calibration, resulting in dynamic parameters obtained, for each step, from the latest updated model.

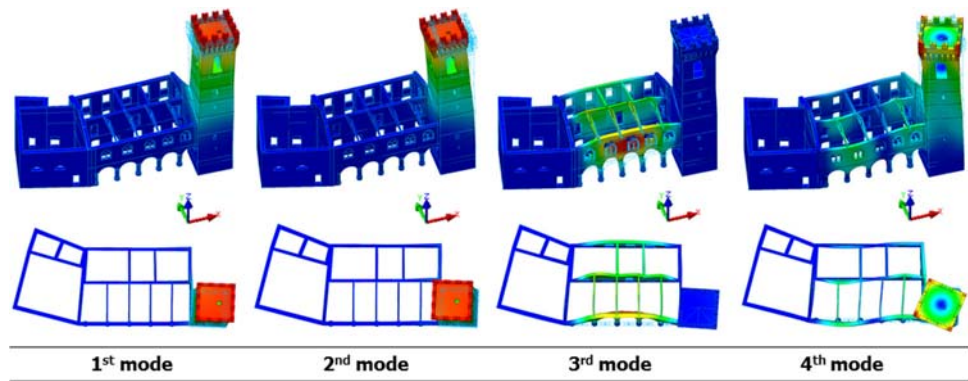
6.1 First step of calibration

The first step of calibration starts considering that the first two modes of both AVS and NM exhibit the same type of the mode shape, as shown in Figs. 8 and 10. This similarity shows that the initial NM is yet quite reliable. However,

Table 3 Modal properties of the initial numerical model (NM)

Mode no.	Frequency (NM) (Hz)	Period (NM) (s)	TRAN-X		TRAN-Y		ROTN-Z		Frequency (AVS) (Hz)	Δf (%)
			Mass(%)	Sum(%)	Mass(%)	Sum(%)	Mass(%)	Sum(%)		
1	1.435	0.697	16.94	16.94	13.2	13.2	0	0	1.491	3.75
2	1.648	0.607	12.58	29.52	16.45	29.64	0	0	1.614	–2.08
3	4.267	0.234	0	29.52	13.87	43.51	5.2	5.2	4.225	–1.00
4	4.816	0.208	0.07	29.59	0.12	43.63	0.01	5.21	5.654	14.81

Fig. 10 The first four modes of the NM: starting point for the calibration



there is still a small difference among frequency values. The first step of calibration aims to reduce these differences. The calibration has been carried out increasing the Young's modulus of the masonry of the palace.

The modulus of Elasticity E was incremented, in the main longitudinal walls of the palace, in order to take into account some recent retrofitting interventions (see Sect. 2). In particular, with reference to correction coefficients reported in Tab C8A.2.2 of [41], for the first elevation of the palace it will be considered a mortar with good characteristics and thin joints. For the second elevation, due to a supposed slightly worse masonry due to an inability to fully investigate the “Pinacoteca” after October 30th, it will be considered—for safety reason—a lower stiffness calculated using only the first coefficient.

The results of the NM are reported in Table 4: a little discrepancy between the first mode of AVS and NM are still present. In fact, it is not sufficient to consider better properties of longitudinal walls with respect to the transversal (damaged) wall of the palace in contact with the tower, and/or a complete disconnection between this transversal wall and the tower in the second elevation. It is also crucial to consider an additional stiffness reduction due to a heavier damage in this transversal wall due to earthquakes (see Fig. 5b–f). Finally, it is central to observe that the decoupling between modes is always present, and they are not the same modes of Fig. 10: the

“Pinacoteca” is involved in the fourth mode and not in the third like in the previous step (Fig. 11).

6.2 Second step of calibration

In this step, a further change of the modulus of elasticity E at different levels of the palace is considered, with the aim of reducing the frequency of the second and of the third modes: this operation has scaled the values of the frequencies, without significant changes in modal shapes, with global improvements in the calibration of the NM. The process has highlighted the fact that the “Pinacoteca” plays an important role in all the four identified modes of AVS.

The calibration has been carried out reducing the Young's modulus around the tower, in particular—as observed in Sect. 6.1—in the transversal walls in contact with the “Pinacoteca”, considering also the possibility of bell cell damage. The Young's modulus was reduced considering a cracked masonry (50% of the initial stiffness with respect to the value of Table 2), where the damage is observable (Fig. 5), even if it is not yet evident as in the bell cell columns and in the area below it (Fig. 12).

At this step of calibration, it is possible to observe that there are quite small differences between the four main frequencies values as reported in Table 5 (last column): of about +3.49% for the first mode, and +2.99% for the second mode and –0.27% for the third mode. The main difference is again on the fourth mode, where a +6.4% is

Table 4 Modal properties after the first calibration of NM

Mode no.	Frequency (NM) (Hz)	Period (NM) (s)	TRAN-X		TRAN-Y		ROTN-Z		Frequency (AVS)(Hz)	Δf (%)
			Mass(%)	Sum(%)	Mass(%)	Sum(%)	Mass(%)	Sum(%)		
1	1.455	0.687	17.47	17.47	11.51	11.51	0	0	1.491	2.43
2	1.693	0.591	10.79	28.25	16.49	28.01	0	0	1.614	–4.89
3	4.662	0.215	0.06	28.31	0.07	28.07	2.31	2.31	4.225	–10.34
4	4.925	0.203	0	28.31	18.44	46.52	0	2.31	5.654	12.90

noticeable comparing the experimental and the numerical frequency. In terms of modal shapes, good matches are observable comparing Figs. 8 and 12.

6.3 Third step of calibration

The last step of the calibration consists of introducing a rigid floor on the Pinacoteca, due to the presence of a rigid r.c. slab at extrados, and to reduce a little bit the stiffness of the masonry tower in the part between the damaged walls (in Fig. 5c, d) and the bell cell [44]. This permits one to consider a more diffuse microcracking (damage) inside the tower. Differently, the stiffness of the “Pinacoteca” longitudinal masonry walls is incremented in order to simulate a further better masonry quality (absence of microcracking or past interventions) with respect to the other parts of the structure.

After this last step of calibration, it is possible to see in Table 6 and in Fig. 13 that the first mode is translational with prevalence in X-direction, and the frequency is equivalent to the one of Table 1 (see the last column of Table 6). The second mode is prevalent in Y-direction with a zero-mass involved in the torsion, and the frequency differs about +0.78% with respect to the measured one. The last two modes, respectively the torsional and now the flexural of the tower with a low participation of the palace, differ about -1.86 and 3.57% with respect to the measured one. The modal shapes are in very good agreement with those extracted by the AVS.

6.4 Discussion on calibration

The complexity of the performed calibration activity is due to the interaction of different structural buildings, giving rise to a construction compound [45]. The performed adjustment is not unique and further changes are possible to make mode shapes of NM more similar to those of AVS. For example, additional steps can be added to eliminate the discrepancy between the third and fourth modes of NM respect to the AVS.

Differently, the periods related to the modes of the NM give us a good feedback on the final calibrated parameters due to the absence of spurious modes and the good participation mass ratio of the considered modes.

By examining Table 1 and Fig. 13, the following comments can be made:

- Within the frequency range 0–6 Hz, four vibration modes were clearly identified.
- The fundamental mode of the bell-tower, with a natural frequency of about 1.49 Hz, involves dominant bending in the N-W direction with significant bending participation in the opposite N-W direction as well; the coupled motion in the two main N–W and N–S directions generally characterizes all tower mode shapes.
- The optimal estimates obtained from the proposed iterative technique provide an important indication on the reliability of the numerical evaluations.
- Both the sets of estimated parameters (stiffness of the masonry and stiffness of the floor) seem to represent very well the damage distribution of the palace and of tower, and are also in good agreement with the cracking appearing after the October 30th earthquake. Specifically, a low stiffness ratio is detected in the wall between the Pinacoteca and the tower, with the Young’s modulus in such regions being about the half of the values obtained in the other parts of the tower (see Table 2). Furthermore, it is possible to conclude that a microcracking developed in the middle part of the tower up to the bell cell, where a half value (with respect to that reported in Table 2) of Young’s modulus is also obtained.
- In the lower part of the tower, the Young’s modulus turns out to be higher in the corner zones than elsewhere. This result is fully consistent with the traditional construction techniques of tower and belfry, generally characterized by the adoption of the best available materials and skills. This situation is also favourite, always in the lower part of the tower, by the

Fig. 11 The first four modes of the NM after the first calibration

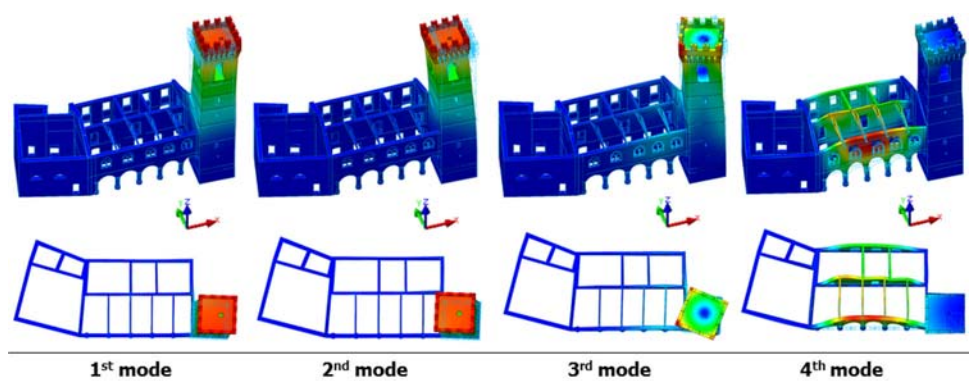


Table 5 Modal properties after the second calibration of NM

Mode no.	Frequency (NM) (Hz)	Period (NM) (s)	TRAN-X		TRAN-Y		ROTN-Z		Frequency (AVS) (Hz)	Δf (%)
			Mass(%)	Sum(%)	Mass(%)	Sum(%)	Mass(%)	Sum(%)		
1	1.439	0.695	13.21	13.21	12.84	12.84	0	0	1.491	3.49
2	1.566	0.639	12.25	25.46	12.56	25.39	0	0	1.614	2.99
3	4.236	0.236	0.1	25.56	0	25.39	3.94	3.94	4.225	-0.27
4	5.292	0.189	6.15	31.72	8.42	33.81	0	3.94	5.654	6.40

Fig. 12 The first four modes of the NM after the second calibration

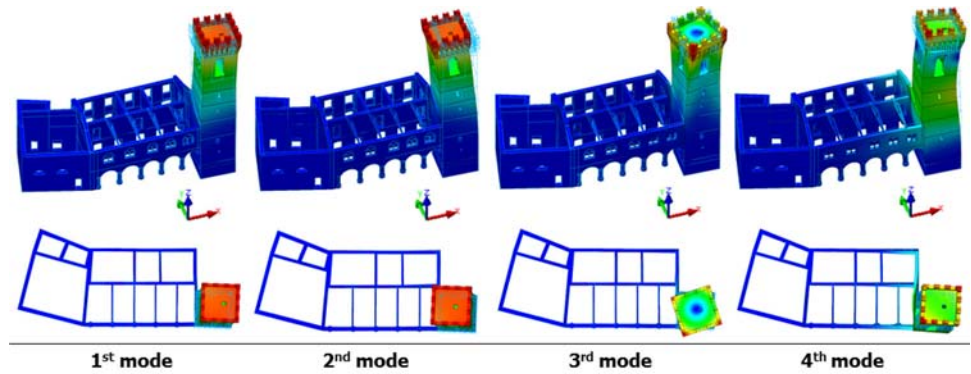
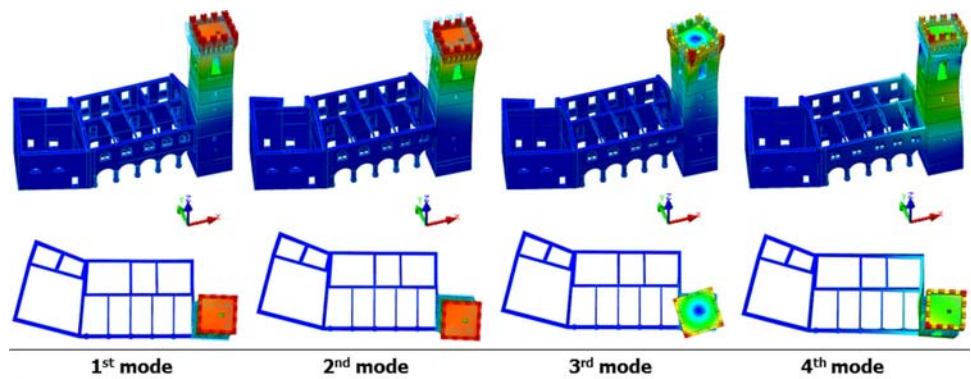


Table 6 The first four modes of the NM after the last step of calibration

Mode no.	Frequency (NM) (Hz)	Period (NM) (s)	TRAN-X		TRAN-Y		ROTN-Z		Frequency (AVS) (Hz)	Δf (%)
			Mass(%)	Sum(%)	Mass(%)	Sum(%)	Mass(%)	Sum(%)		
1	1.492	0.670	12.48	12.48	12.98	12.98	0	0	1.491	-0.07
2	1.601	0.624	12.31	24.79	12.06	25.03	0	0	1.614	0.78
3	4.304	0.232	0.15	24.94	0	25.04	5.4	5.4	4.225	-1.86
4	5.452	0.183	5.57	30.5	9.94	34.97	0	5.4	5.654	3.57

Fig. 13 The first four modes of the NM after the last step of calibration



influence of the axial stresses induced by gravity loads, whose values are often very high.

7 Conclusions

Management, maintenance and preservation of heritage structures usually result in a very complex task because of old construction techniques, unique structural schemes, construction defects and limited destructive investigations for structural characterization. Therefore, the availability of experimental estimations of modal properties becomes relevant for structural and seismic assessment process.

Taking into account the increasing interest towards the opportunities provided by OMA as a tool for the non-invasive techniques, the present study would like to be a contribution to the development of rational and sustainable procedures for non-destructive investigation according to the current codes for seismic protection and rehabilitation of heritage structures.

The modal frequencies, damping ratios and mode shapes of the historical Podestà Palace, Civic Tower and Piety Church of Montelupone, previously damaged by the Italian Earthquakes on 2016 August and October, have been determined by Ambient Vibration Surveys. It is seen that modes are generally formed by partial global displacements, due to the presence of a tower, to the lack of a uniform rigid floor diaphragm, which should require retrofitting interventions like those in [46], and to the absence of a perfect interaction between structural elements, mainly perimeter walls of both the Pinacoteca and the civic tower.

Using the results of experimental study, an accurate NM has been set up. Step by step, imperfect interactions, modulus of elasticity of masonry, stiffness of the floors and masses of secondary elements have been altered. After three steps of NM iterative calibration, numerical results similar to the experimental ones have been obtained.

At all levels, walls have reported scattered values of elastic parameters including the possibility of damages. This is obviously consistent with what happened after the 2016 earthquakes that stroke the central part of the Italy. The lower values of Young's modulus are observed where cracking is actually visible due to the seismic dynamical loads. Differently, this work has allowed to understand where there is the seat of possible damage, mainly micro-cracking and, therefore, further investigations must be carried out in the central part of the tower. Due to the good correlation between experimental and theoretical modal behaviour, the updated models seem to be adequate to provide reliable predictions under the load conditions, interesting to assess the structural safety of the tower and of the palace. Further AVS should be done after the

retrofitting interventions in order to catch the possible diffuse restoration of the palace and of the civic tower. Furthermore, this measure represents an initial assessment of the quality of the proposed retrofitting interventions.

Acknowledgements The authors wish to acknowledge the *Municipal office of Montelupone* (Macerata—Italy), the Mayor Mr. Rolando Pecora, the Head of the technical office Mr. Antonio Spaccesi and the assistant of the technical office Mr. Andrea Pesaola for their valuable helps during the preparation of this work. The authors wish also to acknowledge the *DRC—Diagnostic Research Company* for its support during this work.

References

- Gentile C, Saisi A (2007) Ambient vibration testing of historic masonry towers for structural identification and damage assessment. *Constr Build Mater* 21:1311–1321. doi:10.1016/j.conbuildmat.2006.01.007
- De Stefano A, Matta E, Clemente P (2016) Structural health monitoring of historical heritage in Italy: some relevant experiences. *J Civil Struct Health Monit* 6:83–106. doi:10.1007/s13349-016-0154-y
- Rainieri C, Fabbrocino G, Verderame GM (2013) Non-destructive characterization and dynamic identification of a modern heritage building for serviceability seismic analyses. *NDT&E Int* 60:17–31. doi:10.1016/j.ndteint.2013.06.003
- Ramos LF, Marques L, Lourenço PB et al (2010) Monitoring historical masonry structures with operational modal analysis: two case studies. *Mech Syst Signal Process* 24:1291–1305. doi:10.1016/j.ymsp.2010.01.011
- DPCM (2011) Valutazione e riduzione del rischio sismico del patrimonio culturale con riferimento alle Norme tecniche per le costruzioni di cui al decreto del Ministero delle infrastrutture e dei trasporti del 14 gennaio 2008. S.O. n. 217/L (in Italian)
- Pierdicca A, Clementi F, Isidori D et al (2016) Numerical model upgrading of a historical masonry palace monitored with a wireless sensor network. *Int J Mason Res Innov* 1:74. doi:10.1504/IJMRI.2016.074748
- Pierdicca A, Clementi F, Maracci D et al (2015) Vibration-based SHM of ordinary buildings: detection and quantification of structural damage. In: *ASME Proceedings* (ed) ASME 2015 International design engineering technical conferences & computers and information in engineering conference. American Society of Mechanical Engineers, Boston, pp V008T13A098–V008T13A098
- Pierdicca A, Clementi F, Maracci D et al (2016) Damage detection in a precast structure subjected to an earthquake: a numerical approach. *Eng Struct* 127:447–458. doi:10.1016/j.engstruct.2016.08.058
- Milani G, Valente M (2015) Comparative pushover and limit analyses on seven masonry churches damaged by the 2012 Emilia-Romagna (Italy) seismic events: possibilities of non-linear finite elements compared with pre-assigned failure mechanisms. *Eng Fail Anal* 47:129–161. doi:10.1016/j.engfailanal.2014.09.016
- Acito M, Bocciarelli M, Chesi C, Milani G (2014) Collapse of the clock tower in Finale Emilia after the May 2012 Emilia Romagna earthquake sequence: numerical insight. *Eng Struct* 72:70–91. doi:10.1016/j.engstruct.2014.04.026
- Betti M, Orlando M, Vignoli A (2011) Static behaviour of an Italian Medieval Castle: damage assessment by numerical

- modelling. *Comput Struct* 89:1956–1970. doi:[10.1016/j.compstruc.2011.05.022](https://doi.org/10.1016/j.compstruc.2011.05.022)
12. Catinari F, Pierdicca A, Clementi F, Lenci S (2017) Identification and calibration of the structural model of historical masonry building damaged during the 2016 Italian earthquakes: the case study of Palazzo del Podestà in Montelupone. In: 13th international conference on computational methods for coupled problems in science and engineering—ICCMSE 2017, pp 1–4
 13. Clementi F, Gazzani V, Poiani M et al (2017) Seismic assessment of a monumental building through nonlinear analyses of a 3D solid model. *J Earthq Eng*. doi:[10.1080/13632469.2017.1297268](https://doi.org/10.1080/13632469.2017.1297268)
 14. Cavalagli N, Gusella V (2015) Dome of the Basilica of Santa Maria Degli Angeli in Assisi: static and dynamic assessment. *Int J Archit Herit* 9:157–175. doi:[10.1080/15583058.2014.951799](https://doi.org/10.1080/15583058.2014.951799)
 15. Alvandi A, Cremona C (2006) Assessment of vibration-based damage identification techniques. *J Sound Vib* 292:179–202. doi:[10.1016/j.jsv.2005.07.036](https://doi.org/10.1016/j.jsv.2005.07.036)
 16. Ellis BR (1998) Non-destructive dynamic testing of stone pinnacles on the palace of Westminster. *Proc ICE Struct Build* 128:300–307. doi:[10.1680/istbu.1998.30464](https://doi.org/10.1680/istbu.1998.30464)
 17. Pieraccini M, Dei D, Betti M et al (2014) Dynamic identification of historic masonry towers through an expeditious and no-contact approach: application to the “Torre del Mangia” in Siena (Italy). *J Cult Herit* 15:275–282. doi:[10.1016/j.culher.2013.07.006](https://doi.org/10.1016/j.culher.2013.07.006)
 18. Ubertini F, Cavalagli N, Kita A, Comanducci G (2017) Assessment of a monumental masonry bell-tower after 2016 Central Italy seismic sequence by long-term SHM. *Bull Earthq Eng*. doi:[10.1007/s10518-017-0222-7](https://doi.org/10.1007/s10518-017-0222-7)
 19. Ubertini F, Comanducci G, Cavalagli N et al (2017) Environmental effects on natural frequencies of the San Pietro bell tower in Perugia, Italy, and their removal for structural performance assessment. *Mech Syst Signal Process* 82:307–322. doi:[10.1016/j.ymssp.2016.05.025](https://doi.org/10.1016/j.ymssp.2016.05.025)
 20. Ubertini F, Comanducci G, Cavalagli N (2016) Vibration-based structural health monitoring of a historic bell-tower using output-only measurements and multivariate statistical analysis. *Struct Heal Monit* 15:438–457. doi:[10.1177/1475921716643948](https://doi.org/10.1177/1475921716643948)
 21. Cavalagli N, Comanducci G, Ubertini F (2017) Earthquake-induced damage detection in a monumental masonry bell-tower using long-term dynamic monitoring data. *J Earthq Eng* 13632469(2017):1323048. doi:[10.1080/13632469.2017.1323048](https://doi.org/10.1080/13632469.2017.1323048)
 22. Pierdicca A, Clementi F, Mezzapelle P et al (2017) One-year monitoring of a reinforced concrete school building: evolution of dynamic behavior during retrofitting works. *Procedia Eng* 199:2238–2243. doi:[10.1016/j.proeng.2017.09.206](https://doi.org/10.1016/j.proeng.2017.09.206)
 23. Bartoli G, Betti M, Giordano S (2013) In situ static and dynamic investigations on the “Torre Grossa” masonry tower. *Eng Struct* 52:718–733. doi:[10.1016/j.engstruct.2013.01.030](https://doi.org/10.1016/j.engstruct.2013.01.030)
 24. Zonta D, Glisic B, Adriaenssens S (2014) Value of information: impact of monitoring on decision-making. *Struct Control Heal Monit* 21:1043–1056. doi:[10.1002/stc.1631](https://doi.org/10.1002/stc.1631)
 25. Das S, Saha P, Patro SK (2016) Vibration-based damage detection techniques used for health monitoring of structures: a review. *J Civil Struct Heal Monit* 6:477–507. doi:[10.1007/s13349-016-0168-5](https://doi.org/10.1007/s13349-016-0168-5)
 26. Formisano A (2016) Theoretical and numerical seismic analysis of masonry building aggregates: case studies in San Pio Delle Camere (L’Aquila, Italy). *J Earthq Eng*. doi:[10.1080/13632469.2016.1172376](https://doi.org/10.1080/13632469.2016.1172376)
 27. Doglioni C, Anzidei M, Pondrelli S, Florindo F (2016) The Amatrice seismic sequence: preliminary data and results. *Ann Geophys* 59:1–4. doi:[10.4401/ag-7373](https://doi.org/10.4401/ag-7373)
 28. Lavecchia G, Castaldo R, de Nardis R et al (2016) Ground deformation and source geometry of the 24 August 2016 Amatrice earthquake (Central Italy) investigated through analytical and numerical modeling of DInSAR measurements and structural-geological data. *Geophys Res Lett* 43:12389–12398. doi:[10.1002/2016GL071723](https://doi.org/10.1002/2016GL071723)
 29. Luca S, Billi A, Carminati E et al (2017) Field- to nano-scale evidence for weakening mechanisms along the fault of the 2016 Amatrice and Norcia earthquakes, Italy. *Tectonophysics* 712–713:156–169. doi:[10.1016/j.tecto.2017.05.014](https://doi.org/10.1016/j.tecto.2017.05.014)
 30. Galli P, Peronace E, Brammerini F et al (2016) The MCS intensity distribution of the devastating 24 August 2016 earthquake in central Italy (Mw 6.2). *Ann Geophys*. doi:[10.4401/ag-7287](https://doi.org/10.4401/ag-7287)
 31. Quagliarini E, D’Orazio M, Stazi A (2006) Rehabilitation and consolidation of high-value “camorcanna” vaults with FRP. *J Cult Herit* 7:13–22. doi:[10.1016/j.culher.2005.09.002](https://doi.org/10.1016/j.culher.2005.09.002)
 32. Foti D, Diaferio M, Giannoccaro NI, Mongelli M (2012) Ambient vibration testing, dynamic identification and model updating of a historic tower. *NDT&E Int* 47:88–95. doi:[10.1016/j.ndteint.2011.11.009](https://doi.org/10.1016/j.ndteint.2011.11.009)
 33. Van Overschee P, De Moor B (1996) Subspace identification for linear systems (theory—implementation—applications). Springer, Dordrecht. doi:[10.1007/978-1-4613-0465-4](https://doi.org/10.1007/978-1-4613-0465-4)
 34. Peeters B, De Roeck G (1999) Reference-based stochastic subspace identification for output-only modal analysis. *Mech Syst Signal Process* 13:855–878. doi:[10.1006/mssp.1999.1249](https://doi.org/10.1006/mssp.1999.1249)
 35. Singh JP, Agarwal P, Kumar A, Thakkar SK (2014) Identification of modal parameters of a multistoried rc building using ambient vibration and strong vibration records of Bhuj earthquake, 2001. *J Earthq Eng* 18:444–457. doi:[10.1080/13632469.2013.856823](https://doi.org/10.1080/13632469.2013.856823)
 36. Ewins DJ (1984) Modal testing: theory and practice. Res Stud Press Ltd., Taunton. doi:[10.1098/rsta.2000.0711](https://doi.org/10.1098/rsta.2000.0711)
 37. Van Overschee P, De Moor B (1996) Subspace identification for linear systems. Kluwer, London. doi:[10.1007/978-1-4613-0465-4](https://doi.org/10.1007/978-1-4613-0465-4)
 38. Rainieri C, Fabbrocino G (2011) Operational modal analysis for the characterization of heritage structures. *Geofizika* 28:109–126
 39. Quagliarini E, Maracchini G, Clementi F (2017) Uses and limits of the equivalent frame model on existing unreinforced masonry buildings for assessing their seismic risk: a review. *J Build Eng* 10:166–182. doi:[10.1016/j.jobe.2017.03.004](https://doi.org/10.1016/j.jobe.2017.03.004)
 40. Ministro dei Lavori Pubblici e dei Trasporti (2008) DM 14/01/2008—Norme tecniche per le costruzioni (in Italian). Suppl. Ordin. Gazz. Uff. n. 29
 41. Ministero dei Lavori Pubblici e dei Trasporti (2009) Circolare 2 febbraio 2009, n. 617—Istruzioni per l’applicazione delle “Nuove Norme Tecniche per le Costruzioni” di cui al Decreto Ministeriale del 14/01/2008 (in Italian)
 42. Friswell MI, Mottershead JE (1995) Finite element model updating in structural dynamics. Springer, New York. doi:[10.1007/978-94-015-8508-8](https://doi.org/10.1007/978-94-015-8508-8)
 43. Aras F, Krstevska L, Altay G, Tashkov L (2011) Experimental and numerical modal analyses of a historical masonry palace. *Constr Build Mater* 25:81–91. doi:[10.1016/j.conbuildmat.2010.06.054](https://doi.org/10.1016/j.conbuildmat.2010.06.054)
 44. Krstevska L, Tashkov L, Naumovski N et al (2010) In-situ experimental testing of four historical buildings damaged during the 2009 L’Aquila earthquake. In: COST ACTION C26 urban habitat construction under catastrophic events—proceedings of the final conference, pp 427–432
 45. Formisano A, Florio G, Landolfo R, Mazzolani FM (2015) Numerical calibration of an easy method for seismic behaviour assessment on large scale of masonry building aggregates. *Adv Eng Softw* 80:116–138. doi:[10.1016/j.advengsoft.2014.09.013](https://doi.org/10.1016/j.advengsoft.2014.09.013)
 46. Faggiano B, Marzo A, Formisano A, Mazzolani FM (2009) Innovative steel connections for the retrofit of timber floors in ancient buildings: a numerical investigation. *Comput Struct* 87:1–13. doi:[10.1016/j.compstruc.2008.07.005](https://doi.org/10.1016/j.compstruc.2008.07.005)